Porous Geometry Guided Micro-mechanical Environment Within Scaffolds for Cell Mechanobiology Study in Bone Tissue Engineering

Feihu Zhao [1,2,3], Yi Xiong [4], Keita Ito [1,2], Bert van Rietbergen [1] and Sandra Hofmann [1,2]*

[1]Orthopaedic Biomechanics, Department of Biomedical Engineering, Eindhoven University of Technology, Eindhoven, Netherlands, [2]Institute for Complex Molecular Systems (ICMS), Eindhoven University of Technology, Eindhoven, Netherlands, [3]Zienkiewicz Centre for Computational Engineering, Faculty of Science and Engineering, Swansea University, Swansea, United Kingdom, [4]School of System Design and Intelligent Manufacturing, Southern University of Science and Technology, Shenzhen, China

Mechanobiology research is for understanding the role of mechanics in cell physiology and pathology. It will have implications for studying bone physiology and pathology and to guide the strategy for regenerating both the structural and functional features of bone. Mechanobiological studies *in vitro* apply a dynamic micro-mechanical environment to cells *via* bioreactors. Porous scaffolds are commonly used for housing the cells in a three-dimensional (3D) culturing environment. Such scaffolds usually have different pore geometries (e.g. with different pore shapes, pore dimensions and porosities). These pore geometries can affect the internal micro-mechanical environment that the cells experience when loaded in the bioreactor. Therefore, to adjust the applied micro-mechanical environment on cells, researchers can tune either the applied load and/or the design of the scaffold pore geometries. This review will provide information on how the micro-mechanical environment (e.g. fluid-induced wall shear stress and mechanical strain) is affected by various scaffold pore geometries within different bioreactors. It shall allow researchers to estimate/quantify the micro-mechanical environment according to the already known pore geometry information, or to find a suitable pore geometry according to the desirable micro-mechanical environment to be applied. Finally, as future work, artificial intelligent – assisted techniques, which can achieve an automatic design of solid porous scaffold geometry for tuning/optimising the micro-mechanical environment are suggested.

Keywords: micro-mechanical environment, mechanical stimulation, scaffold porous geometry, mechanobiology, bone tissue engineering

DEFINITION

Scaffold pore geometry that is presented in this review involves the following parameters:

- Pore shape: the architecture or shape of the scaffold micro-pores, which can be irregular or regular (cubic, spherical, gyroid, etc.);
- Pore dimension: also called pore size or pore diameter, which is a measure of the (maximal) distance between two neighbouring struts, usually has a value around 100–2000 μm for bone tissue engineering applications;

- Porosity: also called void fraction, which is a measure of the void (i.e. "empty") spaces in scaffolds, and has a value in the range of 0–100%.

INTRODUCTION

In the field of bone tissue engineering (BTE), a primary challenge is to recapitulate both the structural and functional features of bone (Amini et al., 2012). Mechanobiology research seeks to understand the role of mechanics in cell physiology and pathology. Bone cells are known as mechanosensitive cells that respond to their mechanical environment *in vivo* and *in vitro* (Klein-Nulend et al., 2003; Giorgi et al., 2016). Mechanobiology research in BTE aims at getting insight into how the scaffolds or the application of mechanical loads affect the development of tissue-engineered bone tissue, which is intended to be used for bone disease research, drug testing, etc. (García-Aznar et al., 2021; Kim et al., 2021). *In vitro* mechanobiology includes the creation of either static or dynamic micro-mechanical environments. The cellular mechanical environment is then transduced into biochemical signals through mechano-transduction protein networks, which therefore influence the cellular behaviours, such as osteogenic differentiation of stem cells in BTE (Delaine-Smith and Reilly, 2012; Jansen et al., 2015; Paluch et al., 2015; Wittkowske et al., 2016; Naqvi and McNamara, 2020). A static micro-mechanical environment refers to the use of biomaterials with different mechanical properties to which the cells attach. The effect of mechanical properties inherent to biomaterials on bone cell behaviour have been widely reviewed, e.g. by Janmey et al. (2020), Klein-Nulend et al. (2012), Lin et al. (2020), Selig et al. (2020) or Janmey et al. (2020), to name a few. This review will focus on the dynamic micro-mechanical environment on cells that is guided by the scaffold pore geometry when loading is applied through the use of bioreactors.

Various bioreactors are being applied in BTE. For example, flow perfusion bioreactors, spinner flasks or rotating wall vessels can be used which all apply a fluid induced wall shear stress (WSS) on cells (Granet et al., 1998; Sikavitsas et al., 2002; Bancroft et al., 2003). Mechanical compression and stretching bioreactors can be used for applying mechanical strain to cells that are attached on scaffold struts (Zhang et al., 2008; Bilgen et al., 2013). For cell culturing in 3D, scaffolds are used for housing and supporting the seeded cells. Scaffolds used in the experiments usually have different porous geometries, for example some have irregular pore shapes (Mccoy et al., 2012), and some have regular pores but with different porosities or pore dimensions (Bartnikowski et al., 2014). With improvements in 3D printing/additive manufacturing technology, scaffolds with well-defined geometries can be manufactured, and this will probably be the standard for scaffold manufacturing in the near future (Bahraminasab, 2020). To investigate the influence of scaffold pore geometry on the internal micro-mechanical environment, computational approaches are commonly used, thanks to the capability of such approaches to calculate/simulate the mechanical environment at the micro (or even

sub-micro) scale with low cost, which is challenging for experimental measurements (García-Aznar et al., 2021). It has been found that the scaffolds' pore geometry can largely influence the micro-mechanical environment within the scaffolds (Olivares et al., 2009). Previous examples are the computation of the fluid flow induced micro-mechanical environment when applying flow perfusion-, spinner flask- or rotating wall vessel bioreactors by the application of computational fluid dynamics (CFD). Or the mechanical deformation (such as stretching/compression) of the cells within scaffolds in compression/stretching bioreactors (Brunelli et al., 2017), where finite element (FE) models based on fluid-structure interaction (FSI), biphasic poro-elasticity, etc. have been used for simulating/quantifying the resultant WSS and/or mechanical strain on scaffold struts (Zhao et al., 2016; Castro and Lacroix, 2018).

This review aims at providing insight into the role of scaffold pore geometry parameters (i.e. porosity, pore dimension and pore shape) based on previous theoretical studies, in order to better understand their complex effect on the micro-mechanical environment of bone cells. It will benefit the BTE/bone organoids fields for cellular mechanobiology research. For example, this information is expected to allow researchers to estimate the micro-mechanical environment depending on scaffold geometry information, or to find/design a suitable pore geometry providing a desirable micro-mechanical environment to the cells. The limitations of the current computational approaches in automatically achieving a scaffold geometry design that is driven by micro-mechanical environment will be discussed. An outlook and suggestions for future research in terms of artificial intelligence (AI) – assisted techniques for addressing the limitations in scaffold geometry design will be presented.

THE ROLE OF SCAFFOLD PORE GEOMETRY ON THE CELL MICRO-MECHANICAL ENVIRONMENT

This section will present the influence of the scaffold pore geometry, more specifically pore shape, pore dimension and porosity on the resultant WSS and mechanical strain within empty scaffolds in perfusion, spinner flask and compression bioreactors.

Assumptions for Calculating the Cell Micro-mechanical Environment Within Scaffolds

The calculation of fluid – induced WSS within empty scaffolds is based on the assumption that the WSS at the scaffold surface is a good representation of the WSS sensed by the cells that are attached to the scaffold surfaces. It also assumes that the cells attach mostly flat to the scaffold surface in the initial state, with a minimal cell volume with respect to the pore volume. This assumption has been shown to be met for some experiments/scaffold materials (**Figure 1A**), but not for all (**Figure 1B**). For calculating the mechanical strain in empty scaffolds, it is assumed
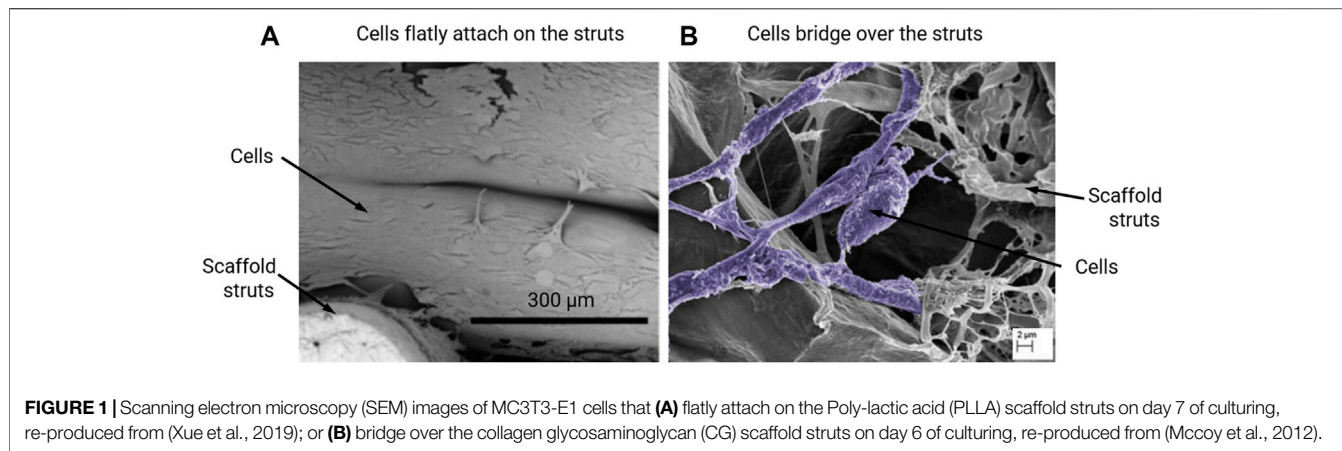
FIGURE 1 | Scanning electron microscopy (SEM) images of MC3T3-E1 cells that **(A)** flatly attach on the Poly-lactic acid (PLLA) scaffold struts on day 7 of culturing, re-produced from (Xue et al., 2019); or **(B)** bridge over the collagen glycosaminoglycan (CG) scaffold struts on day 6 of culturing, re-produced from (Mccoy et al., 2012).
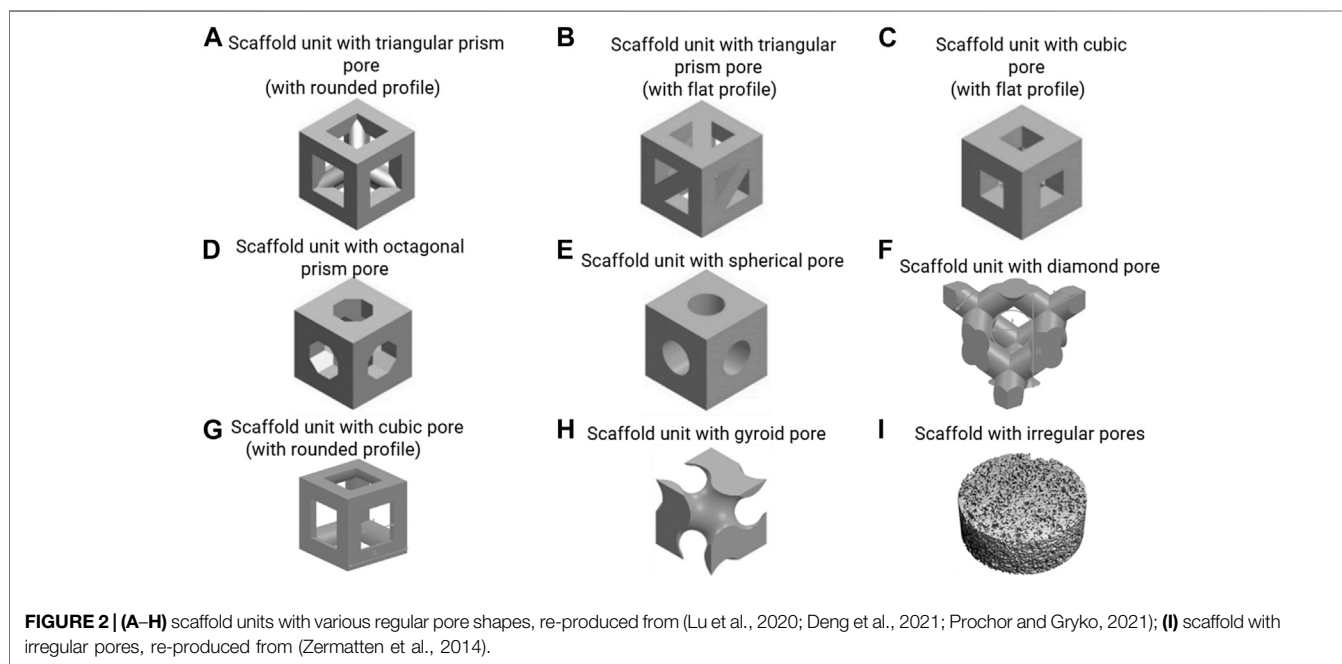
FIGURE 2 | (A–H) scaffold units with various regular pore shapes, re-produced from (Lu et al., 2020; Deng et al., 2021; Prochor and Gryko, 2021); **(I)** scaffold with irregular pores, re-produced from (Zermatten et al., 2014).

that the cells are subjected to the strain magnitude at the location of the scaffold that they are attached to (Olivares et al., 2009; Laurent et al., 2014). Such assumptions can be reasonable if the scaffold material is much stiffer than the cell and no substantial ECM has been formed yet.

Porosity

Porosity is the main determinant for scaffold permeability and thus the amount of flow through the scaffold in perfusion/stirring bioreactors and was found to be an important parameter determining the results of BTE (e.g. seeded cell density, cell proliferation, ECM production, etc.) (Grayson et al., 2008; Panseri et al., 2021). The effect of porosity on the permeability of the scaffold, which describes the amount of flow through the scaffold, can be calculated by the Kozeny-Carman Equation (**Eq. 1**) (Van Bael et al., 2012; Egan, 2019):

$$\kappa = \left(\frac{1}{C_k}\right) \cdot \frac{\varphi}{S_s^2} \tag{1}$$

where, κ is the permeability, φ is the porosity, c_k is the Kozeny constant and S_s is the specific surface area calculated as the surface area divided by the total volume of the struts.

This equation demonstrates that scaffold permeability linearly increases with porosity. This has also been demonstrated by experimental measurements (Zhang et al., 2019). The relationship between the permeability, the fluid velocity and the WSS, however, is complex and also depends on the pore geometry. Ali and Sen (2018) employed a CFD approach to investigate the influence of porosity on the permeability and WSS, and they found that under a fluid velocity of 0.7 mm/s, the average WSS decreased from 131 to 27 mPa with an increase in porosity from 65 to 90% for the gyroid pore shape (**Figure 2H**).

This trend also happened for a diamond pore shape (**Figure 2F**) (Ali and Sen, 2018). Melchels et al. (2011) designed and manufactured a scaffold (gyroid pores in **Figure 2H**) with different porosities (40–85%) in different regions. This resulted in different shear rates (SRs) in the regions with different porosities under perfusion flow, e.g. 10–40 s^{-1}, i.e. higher SR in the region with higher porosity (Melchels et al., 2011).

Porosity is also the main determinant for the amount of strain in the scaffold when an external force is applied according to both micro-FE analyses and experimental characterisation (Hannink and Arts, 2011; Castro et al., 2020). If under pressure/compressive force loading through bioreactors, a scaffold with a lower porosity (i.e. higher overall structural stiffness) will show less deformation, thus cells that attach on the struts will receive lower strain. Not only for overall structural stiffness, the porosity also can influence the local stress/strain concentration under compression loading. For instance, in the computational study by Hendrikson et al. (2017), scaffolds that had a cubic pore shape, a pore dimension of 151 μm, but different porosities (74 vs 64%) were compared in terms of octahedral shear strain under a compressive strain of 10%. It was found that the scaffold with higher porosity (74%) had a larger strut area in the low strain range (e.g. <10%) than the one with lower porosity (64%) (Hendrikson et al., 2017). Similarly to **section 2.2 and 2.3**, under dynamic compression, the porosity will also have an influence on the resultant WSS that is induced by fluid flow due to compression. Zhao et al. (2016) compared scaffolds with porosities of 60–90% and found that a higher porosity resulted in lower WSS under dynamic compression. By increasing the pore dimension, the influence of porosity on WSS became smaller, e.g. for cubic pore, dimension = 100 μm: average WSS = 3.5 mPa when porosity = 60%, average WSS = 2.5 mPa when porosity = 90%; for cubic pore, dimension = 300 μm: average WSS = 1.5 mPa when porosity = 60%, average WSS = 1.1 mPa when porosity = 90% under dynamic compression (strain = 1%, frequency = 1 Hz) (Zhao et al., 2016). So, under dynamic compression, the lower porosity and pore dimension can result in higher fluid flow-induced WSS.

Pore Dimension

Pore dimension is the main factor that determines fluid-induced WSS under perfusion flow (Fu et al., 2021). Also, pore dimension is one of the factors that can influence cell attachment (e.g. flatly attached on struts/bridging over struts in **Figure 1**) (Guo et al., 2015; Yamashita et al., 2016). Previous mechanobiological studies have investigated cell responses via tuning the scaffold pore dimensions while keeping the pore shape constant (Bartnikowski et al., 2014; Ouyang et al., 2019). For example, Bartnikowski et al. (2014) quantified the WSS within the scaffolds that had cubic pores (with rounded profile in **Figure 2G**) and a porosity of 60% but with different pore dimensions (625 vs 1250 μm). It was found that the scaffold with smaller pore dimension provided a higher WSS: maximum WSS = 1979 mPa/average WSS = 500 mPa (pore dimension = 625 μm) vs maximum WSS = 837 mPa/average WSS = 120 mPa (pore dimension = 1250 μm) under a flow rate of 1 ml/h (0.61 μm/s). These scaffolds were then applied in an *in vitro* cell experiment where it was found that the DNA amount was

significantly higher in the cell seeded scaffold with larger pore dimension (1250 μm) (Bartnikowski et al., 2014). Whereas the accurate calculation of the actual WSS requires performing a CFD analysis for the (often complex) scaffold pore geometries, simple mathematical equation can be used to estimate the WSS (Zhao et al., 2016):

$$\frac{\tau_a}{v} = a_1 \cdot \left(\frac{d}{L_c}\right)^{b_1} \tag{2}$$

Where, τ_a is the average WSS within the scaffold, v the applied fluid velocity, d the pore dimension, L_c is the characteristic length ($L_c = 1$ μm), and a_1 and b_1 constants that depend on the pore shape and porosity. A limitation of this approach is that the equations are only a good approximation for a limited set of pore shapes (i.e. cube with flat profile and sphere in **Figures 2C,E**) and porosities (i.e. 60%–90%).

Dynamic compression not only generates mechanical strains in the struts but can also result in WSS on the strut surfaces, which was mostly ignored in previous mechanobiological studies regardless of the compressive strain magnitude or frequency. It was found that the resultant average WSS was proportional to the applied compressive strain (Milan et al., 2009). Moreover, it was highly dependent on the scaffold pore dimensions (Zhao et al., 2016). Here also, simple equations were introduced to estimate the WSS due to compression (Zhao et al. (2016)):

$$\frac{\tau_a}{\varepsilon_{app}} = a_2 \cdot \left(\frac{d}{L_c}\right)^{b_2} \tag{3}$$

where, τ_a is the average WSS within the scaffold, ε_{app} is the applied compressive strain by bioreactor, d the pore dimension, L_c is the characteristic length ($L_c = 1$ μm), and a_2 and b_2 constants that depend on the pore shape and porosity. Similar as in **Eq. 2**, one of the limitations of this approach is that the equations are a good approximation only for a limited set of pore shapes (i.e. cube with flat profile and sphere in **Figures 2C,E**) and porosities (i.e. 60%–90%). Also, this **Eq. 3** is only applicable for a dynamic compression frequency of 1.0 Hz and needs to be adapted to other frequencies. For all other cases beyond the aforementioned ones, a FSI analyses will be needed to accurately calculate the WSS.

Under mechanical compression, the stress/strain distribution can be influenced by the pore dimension. Ribeiro et al. (2017) investigated this based on the scaffolds with pore dimensions of 740 and 370 μm using an FE model. There, an unconfined compression loading with a strain of 15% was applied on both scaffolds. Their results showed that the maximum value of compressive stress was similar between the two scaffolds with different pore dimensions, i.e. maximum compressive stress = 27.7 MPa in pore dimension of 740 μm vs maximum compressive stress = 25.9 MPa in pore dimension of 370 μm. However, the scaffold with larger pores (pore dimension = 740 μm) had more regions (area) with higher stress than the one with smaller pores (pore dimension = 370 μm) (Panadero et al., 2015).

Pore Shape

The effect of pore shape on the fluid-induced WSS in flow perfusion and spinner flask bioreactors is difficult to predict. Some scaffolds with different regular pore shapes (but same pore size and porosity) have similar WSS, but some do not. The commonly (designed) regular pore shapes include sphere, cube, gyroid, prism, etc. (**Figures 2A–H**), which can be manufactured by 3D printing/additive manufacturing technology. Prochor and Gryko (2021) quantified the WSS within scaffolds that have different regular pore shapes (e.g. triangular prism with rounded and flat profiles, cube, octagonal prism and sphere in **Figures 2A–E**) under perfusion flow. It was found that the scaffold with triangular prism (with rounded profile) experienced the highest WSS, whereas the scaffold with spherical pores experienced the lowest WSS under the same flow rate. The maximum WSS within spherical pores and cubical pores were identical. However, this can be different within different bioreactors that generate fluid – induced WSS. In a combined experimental and computational BTE study by Rubert et al. (2020), the average WSS within the scaffolds with spherical pores (average pore diameter = 330 μm, porosity = 84.7%) and cubical pores (average pore diameter = 330 μm, porosity = 92.8%) were 0.42 and 0.81 mPa respectively in a spinner flask (70 RPM). This was associated to upregulated osteoblast cell differentiation and ECM formation within cubic pores, while ECM mineralisation was enhanced within the spherical pores (Rubert et al., 2020).

Porous scaffolds also can have irregular pore shapes, which are for example obtained from more traditional fabrication methods such as porogen leaching (**Figure 2I**). Studies have found that the irregularity of the pore shape does not have a distinct influence on the fluid – induced WSS, once the pore dimensions and porosity are similar. For example, Zermatten et al. (2014) investigated the influence of the pore irregularity on the internal WSS using scaffolds with regular cubical pores (with rounded profile) and highly irregular pores (**Figures 2G,I**). Although the other two parameters, pore dimensions (regular: 0.22 mm vs irregular: 0.16 mm) and porosity (regular: 38% vs irregular: 55%) were not exactly the same, the average WSS within irregular and irregular pores have high similarity (regular: 3.08 mPa vs irregular: 3.68 mPa) under a perfusion fluid velocity of 0.066 mm/s (Zermatten et al., 2014). One limitation of simulating the micro-fluidic environment within these highly irregular pores (at whole scaffold level) was the high computational cost (Santamaría et al., 2013; Zermatten et al., 2014). To address this challenge, Zhao et al. (2019) developed a more versatile technique, creating a multiscale and multiphasic CFD model. In this approach, small but representative parts of the scaffold are being used for the generation of a microstructural model of the pore environment, which are then coupled with a macro-model representing the whole scaffold in which the microstructure is homogenised. The macro-model can be used to calculate the fluid flow at larger length scales, that then can be applied to the micro-model to calculate the local WSS at the cell level. As only small parts of the scaffold need to be modelled in detail, this approach can reduce the computational costs while still providing results at the cell-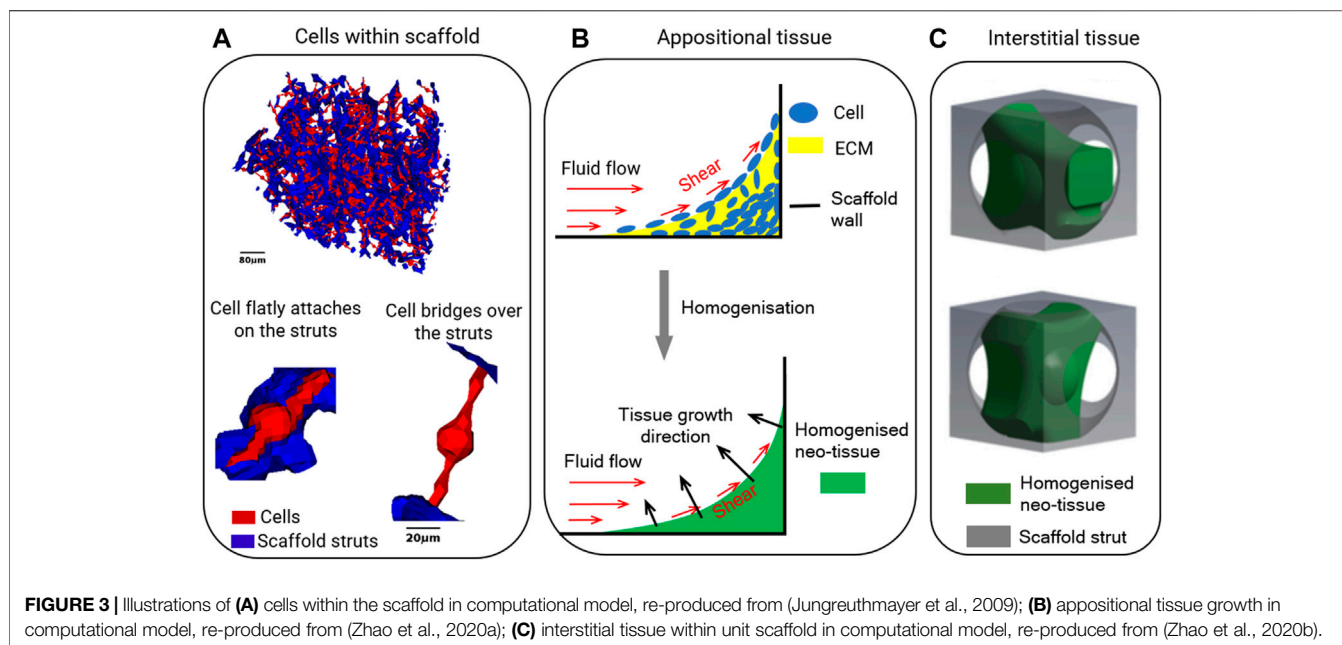level. It has been shown that with this multiscale and multiphasic CFD model, calculations of resulting WSS within any scaffold with highly irregular pore shape is possible even using a normal computer (e.g. 16 GB RAM, Intel i7 CPU). However, this technique requires that the Reynolds (Re) number should less than 1 when using Darcy's law for homogenisation (Chaudhary et al., 2011).

Under mechanical compression, the pore shape can have a distinct influence on the overall structural stiffness of the scaffold (Castro et al., 2020; Jahir-Hussain et al., 2021). According to their calculations, the triangular pore shape resulted in the highest structural stiffness of the scaffold and the spherical pore shape resulted in the lowest stiffness among the various pore shapes (spherical, cubic, hexagonal and triangular). Under pressure/compressive force, scaffolds with a lower structural stiffness (e.g. with spherical pores) will have a higher strain in the struts than the ones with a higher structural stiffness (e.g. with cubic/hexagonal/triangular pores). This difference will translate to differences in strain sensed by cells attached to the struts. In cell culture experiments applying compression to stimulate cells, usually dynamic compression is applied. As mentioned in **sections 2.2 and 2.3**, this dynamic compression also generates WSS within the pores of the scaffold. A FSI approach for quantifying the WSS during dynamic compression has found that the WSS was higher within spherical pores than that within cubical pores, e.g. 5.5 mPa within spherical pores (pore diameter = 100 μm, porosity = 60%) and 3.5 mPa within cubical pores (pore diameter = 100 μm, porosity = 60%) under an applied compressive strain of 1.0% and at a frequency of 1.0 Hz (Zhao et al., 2016). Therefore, to precisely quantify the WSS due to dynamic compression, the pore shape needs to be explicitly reflected in the computational model.

Some scaffolds have extremely anisotropic pores, such as those with unidirectional channels or holes, as shown in (Deville et al., 2006, 2007; Munch et al., 2009; Pourhaghgouy et al., 2016). For this type of scaffolds, the above discussed influence of porosity, pore dimension and pore shape on the internal micro-mechanical environment is still applicable for external loading in the unidirectional orientation (e.g. fluid perfusion/unidirectional mechanical compression/stretching), but not for external loading in non-unidirectional directions (e.g. spinner flask/non-unidirectional compression/stretching).

EFFECT OF CELL/TISSUE GROWTH ON THE MICRO-MECHANICAL ENVIRONMENT WITHIN SCAFFOLD PORES

A major limitation of all studies above is that they do neither consider the cells nor the tissue within the scaffold pores. In these studies, it is assumed that the cells lie flatly attached to the scaffold surface and that their volume is small compared to the pore volume. In other situations, e.g. when cells can bridge across the pores (**Figure 1B**) (Mccoy et al., 2012), this assumption no longer holds and can lead to large errors when calculating the WSS. Moreover, once tissue starts to form within the scaffold, its

FIGURE 3 | Illustrations of **(A)** cells within the scaffold in computational model, re-produced from (Jungreuthmayer et al., 2009); **(B)** appositional tissue growth in computational model, re-produced from (Zhao et al., 2020a); **(C)** interstitial tissue within unit scaffold in computational model, re-produced from (Zhao et al., 2020b).

porosity, and consequently the micro-mechanical environment, can dramatically change (Sandino and Lacroix, 2011). The influence of scaffold pore geometry on the micro-mechanical environment when considering cell/tissue growth has not been as rigorously investigated as within empty scaffolds. In this section, some computational models which can simulate the micro-mechanical environment while considering cell/tissue within scaffolds are reviewed.

Cells Within Scaffold Pores

In some BTE experiments, dynamic cell seeding is used for improving the seeding efficiency and/or distribution of seeded cell in the porous scaffolds. Perfusion flow is usually used for dynamic seeding. During this process, the fluid force can also mechanically stimulate the cells through cell deformation which consequently can promote cellular processes (Rüberg and Aznar, 2016; Serrano-Alcalde et al., 2017).

For seeded cells, Jungreuthmayer et al. (2009) and Mccoy et al. (2012) modelled cells as flatly attached and as bridged morphologies within collagen glycosaminoglycan (CG) scaffolds, which had irregular pore shapes (**Figure 3A**). It was found that the influence of cell morphology (attached/bridged) on the cellular WSS depends on the locations within scaffolds (Guyot et al., 2016b). Furthermore, in the study by Mccoy et al. (2012), three CG scaffolds with different pore dimensions (85, 120 and 325 μm) but equal porosity (90%) were compared in terms of resultant WSS on cells. It was found that the average WSS on all cells (both bridged and attached morphologies) was 165, 176 and 155 mPa, respectively for the pore dimensions of 85, 120 and 325 μm under a perfusion fluid velocity of 235 μm/s, and the WSS was proportional to the fluid velocity (Mccoy et al., 2012).

Tissue Growth Within Scaffold Pores

To investigate the influence of scaffold pore geometry on the changing micro-mechanical environment over time, tissue growth models have been introduced. These are coupled with FE/CFD models. To account for tissue growth, various studies have developed mathematical models to describe neo-tissue formation assuming appositional growth in static conditions (Nava et al., 2013; Guyot et al., 2014; Herklotz et al., 2015; Egan et al., 2018). In the mathematical model, the cells and ECM are usually homogenised (**Figure 3B**). One of the most commonly used models for describing the tissue growth kinetics is based on the level set (LS) method, which is available in both commercial and open-source software packages (e.g. COMSOL, ANSYS, OPENFOAM, etc.). It allows to model appositional tissue growth as illustrated in **Figure 3B**. The governing equation is (Guyot et al., 2014):

$$\frac{\partial \psi}{\partial t} + (V_G \cdot \mathbf{n_\Gamma}) \cdot \nabla \psi = 0 \qquad (4)$$

where, $\mathbf{n_\Gamma}$ is the normal unit vector to the interface between neo-tissue and medium domains, ψ is the LS function and V_G is neo-tissue growth velocity governed by local the struts curvature κ_c in **Eq. 5**:

$$V_G = \begin{cases} -\lambda \cdot \kappa_c & (\kappa_c > 0) \\ 0 & (\kappa_c \leq 0) \end{cases} \qquad (5)$$

Where, λ is the tissue growth rate.

To investigate the influence of the micro-mechanical environment changes during neo-tissue growth within scaffolds that have different pore geometries, the tissue growth model needs to be coupled with the FE/CFD model by introducing a WSS-dependent term into **Eq. 5**. The WSS (τ)

in **Eqs 6**, **7** by Guyot et al. (2015, 2016a) then is computed by a CFD model:

$$V_G = \begin{cases} -A \cdot \kappa \cdot f(\tau) & \kappa > 0 \\ 0 & \kappa \leq 0 \end{cases} \qquad (6)$$

$$f(\tau) = \begin{cases} 0.5 + \dfrac{0.5\tau}{a_1} & 0 \leq \tau \leq a_1 \\ 1 & a_1 \leq \tau \leq a_2 \\ \dfrac{\tau - a_3}{a_2 - a_3} & a_2 \leq \tau \leq a_3 \\ 0 & \tau \geq a_3 \end{cases} \qquad (7)$$

Where, a_1 and a_2 are the minimal and maximal shear stresses enhancing neo-tissue formation and a_3 the critical shear stress.

Then the computational model is applied to scaffolds that have different pore geometries. For instance, Guyot et al. (2015) applied the model on scaffolds with two different pore shapes (i.e. cubic shape with rounded profile and pore dimensions of 650 μm vs diamond shape and pore dimension of 750 μm in **Figures 2F,G**). It was found that under the same amount of tissue produced within the scaffolds higher shear stress occurred in the neo-tissue within the scaffold with diamond shape than that in the scaffold with cubic shape, e.g. when 30% of the porous volume was filled with neo-tissue, the average shear stress in the neo-tissue was 175 mPa within the diamond pores, while it was 80 mPa within the cubic pores (Guyot et al., 2015).

One of the limitations of these computational models is the uncertainty of the parameter values (such as λ, a_1, a_2 and a_3 in **Eqs 5–7**). As these are empirically determined constants, they may need to be changed depending on parameters that influence tissue formation (e.g. the number of cells in the culture, the type of cells, scaffold-related attachment of cells, the density of the deposited ECM and whether or not it is mineralised). Whereas after fitting these constants to experimental results these equations thus may well describe the effect of changes made within that specific experiment, they may not well describe the outcome of other experiments. To reduce the number of parameters in the tissue growth model, recent computational studies have employed second order diffusion equations to model tissue growth kinetics (Buenzli et al., 2020; Zhao et al., 2020a). The main advantage of using this diffusion equations over the LS method is that fewer parameters need to be determined. For example, diffusion equations can already model the curvature – dependent tissue growth without adding the curvature parameter κ in the equation as that in LS method (Buenzli et al., 2020). Therefore, in modelling the scaffold pore geometry for tissue growth kinetics, if the curvature is not a parameter that needs to be explicitly assessed, a computational model based on a diffusion equation will be a good choice. Otherwise, a computational model based on LS method is suggested. Another limitation is that these computational models assume appositional tissue formation towards the centre of the pores. In reality, however, interstitial formation, in which the tissue is infiltrated within the pores rather than being attached on the struts surfaces is also observed in many cases (Li et al., 2009) (as illustrated in **Figure 3C**). The resultant WSS on cells under interstitial tissue formation was quantified and compared to appositional tissue formation (Zhao et al., 2020b). Distinct difference in WSS between two cases were found, even if the same amount of newly formed tissue was present. This implies that computational models that assume appositional tissue growth cannot well predict the micro-mechanical environment in case of substantial interstitial tissue formation. Estimating the influence of scaffold pore geometry on the micro-mechanical environment by taking the tissue into account also needs to consider whether the cell/tissue growth is appositional or interstitial. Even then, this remains challenging due to the high variability in tissue formation.

Different from LS method and diffusion equation, some other computational studies employed a simple voxel – FE based method to simulate the tissue growth within scaffolds (Adachi et al., 2006; Nasello et al., 2021). In this method, modelling the neo-tissue generation within scaffolds was achieved by adding elements on the scaffold surfaces according to the applied stress in elements where the cells are located. Therefore, this voxel – FE based method does not require mathematical functions for tissue growth kinetics. However, this method is limited to simulate the neo-tissue growth under mechanical stimulation only, and not under static conditions.

OUTLOOK

This review provides an insight on how scaffold pore geometry influences the micro-mechanical environment within scaffold pores, i.e. the environment that cells are subjected to. This information would allow researchers to estimate/quantify the micro-mechanical environment according to the already known pore geometry information, or to find a suitable pore geometry according to the desirable micro-mechanical environment to be applied. It also indicates which computational technique could be used for modelling the scaffold in each specific circumstance (e.g. under perfusion flow/spinner flask/compression). So far, these investigations are still in their infancy, in which a large number of scaffold geometries need to be computationally modelled, from which then the users can select suitable ones. A truly automatic optimisation of the scaffold design would obviously involve a much more rigorous approach involving search algorithms. Considering the large number of variables involved, the complexity of the design space, and the time-dependent behaviour of the problem, classical optimisation procedures are not well suited for this task. New techniques, such as an AI-assisted design pipeline centred around the computational methods/tools) could be used for addressing these limitations. To establish an AI-assisted design pipeline, several steps are needed. First, a generative computer-aided design method that can model both periodic and stochastic scaffolds will be needed to greatly enlarge the design space (Tang et al., 2020). These scaffolds with complex biomimetic designs may possess enormous potential to advance the performance of mimicking the *in vivo* condition.

Second, model order reduction methods, which have been used for designing additive manufacturing products (e.g. by Xiong et al. (2019)) are needed to speed up the computer simulations, such that large training sets become available. Third, a systematic method to determine the relationship between multiple factors (e.g. scaffold geometry parameters, mechanical properties of scaffold material, chemical composition, cell attachment sites etc.) during the experimental cell mechanobiology study are needed for developing an AI-assisted design pipeline. To do this, we suggest a combination of experimental methods (e.g. adaptive sampling) and a data-driven modelling approach, which will enable the application of more advanced tasks, such as multi-task/purpose and active learning. After training, it then would be possible to suggest an optimal scaffold for a specified set of requirements with no or minimal additional computational analyses.

AUTHOR CONTRIBUTIONS

FZ, SH, BR, and KI contributed to the design of this review. FZ wrote the draft, in which YX wrote the contents related to the artificial intelligence assisted design. YX also had an overall check of the draft. FZ, SH, BR, and KI contributed to the manuscript revision and read. All authors approved the submitted version.

FUNDING

REFERENCES

Acosta Santamaría, V. A., Malvè, M., Duizabo, A., Mena Tobar, A., Gallego Ferrer, G., García Aznar, J. M., et al. (2013). Computational Methodology to Determine Fluid Related Parameters of Non Regular Three-Dimensional Scaffolds. *Ann. Biomed. Eng.* 41, 2367–2380. doi:10.1007/s10439-013-0849-8

Adachi, T., Osako, Y., Tanaka, M., Hojo, M., and Hollister, S. J. (2006). Framework for Optimal Design of Porous Scaffold Microstructure by Computational Simulation of Bone Regeneration. *Biomaterials* 27, 3964–3972. doi:10.1016/j.biomaterials.2006.02.039

Ali, D., and Sen, S. (2018). Permeability and Fluid Flow-Induced wall Shear Stress of Bone Tissue Scaffolds: Computational Fluid Dynamic Analysis Using Newtonian and Non-newtonian Blood Flow Models. *Comput. Biol. Med.* 99, 201–208. doi:10.1016/j.compbiomed.2018.06.017

Amini, A. R., Laurencin, C. T., and Nukavarapu, S. P. (2012). Bone Tissue Engineering: Recent Advances and Challenges. *Crit. Rev. Biomed. Eng.* 40, 363–408. doi:10.1615/CritRevBiomedEng.v40.i5.10

Bahraminasab, M. (2020). Challenges on Optimization of 3D-Printed Bone Scaffolds. *Biomed. Eng. Online* 19, 1–33. doi:10.1186/s12938-020-00810-2

Bancroft, G. N., Sikavitsas, V. I., and Mikos, A. G. (2003). Technical Note: Design of a Flow Perfusion Bioreactor System for Bone Tissue-Engineering Applications. *Tissue Eng.* 9, 549–554. doi:10.1089/107632703322066723

Bartnikowski, M., Klein, T. J., Melchels, F. P. W., and Woodruff, M. A. (2014). Effects of Scaffold Architecture on Mechanical Characteristics and Osteoblast Response to Static and Perfusion Bioreactor Cultures. *Biotechnol. Bioeng.* 111, 1440–1451. doi:10.1002/bit.25200

Bilgen, B., Chu, D., Stefani, R., and Aaron, R. K. (2013). Design of a Biaxial Mechanical Loading Bioreactor for Tissue Engineering. *JoVE* 74, e50387. doi:10.3791/50387

Brunelli, M., Perrault, C. M., and Lacroix, D. (2017). Short Bursts of Cyclic Mechanical Compression Modulate Tissue Formation in a 3D Hybrid Scaffold. *J. Mech. Behav. Biomed. Mater.* 71, 165–174. doi:10.1016/j.jmbbm.2017.03.008

Buenzli, P. R., Lanaro, M., Wong, C. S., Mclaughlin, M. P., Allenby, M. C., Woodruff, M. A., et al. (2020). Cell Proliferation and Migration Explain Pore Bridging Dynamics in 3D Printed Scaffolds of Different Pore Size. *Acta Biomater.* 114, 285–295. doi:10.1101/2020.03.12.989053

Castro, A. P. G., and Lacroix, D. (2018). Micromechanical Study of the Load Transfer in a Polycaprolactone-Collagen Hybrid Scaffold when Subjected to Unconfined and Confined Compression. *Biomech. Model. Mechanobiol.* 17, 531–541. doi:10.1007/s10237-017-0976-5

Castro, A. P. G., Santos, J., Pires, T., and Fernandes, P. R. (2020). Micromechanical Behavior of TPMS Scaffolds for Bone Tissue Engineering. *Macromol. Mater. Eng.* 305, 1–10. doi:10.1002/mame.202000487

Chaudhary, K., Cardenas, M. B., Deng, W., and Bennett, P. C. (2011). The Role of Eddies inside Pores in the Transition from Darcy to Forchheimer Flows. *Geophys. Res. Lett.* 38. doi:10.1029/2011GL050214

Chunqiu, Z., Xin, D., Han, W., Weimin, Z., and Dong, Z. (2008). Perfusion-compression Bioreactor as the Optimum Choice for Growing Large-Sized Engineered Bone Constructs In Vitro. *Biosci. Hypotheses* 1, 319–323. doi:10.1016/j.bihy.2008.05.008

Delaine-Smith, R. M., and Reilly, G. C. (2012). Mesenchymal Stem Cell Responses to Mechanical Stimuli. *Muscles. Ligaments Tendons J.* 2, 169–180.

Deville, S., Saiz, E., and Tomsia, A. P. (2006). Freeze Casting of Hydroxyapatite Scaffolds for Bone Tissue Engineering. *Biomaterials* 27, 5480–5489. doi:10.1016/j.biomaterials.2006.06.028

Deville, S., Saiz, E., and Tomsia, A. P. (2007). Ice-templated Porous Alumina Structures. *Acta Materialia* 55, 1965–1974. doi:10.1016/j.actamat.2006.11.003

Egan, P. F. (2019). Integrated Design Approaches for 3D Printed Tissue Scaffolds: Review and Outlook. *Materials* 12, 2355. doi:10.3390/ma12152355

Egan, P. F., Shea, K. A., and Ferguson, S. J. (2018). Simulated Tissue Growth for 3D Printed Scaffolds. *Biomech. Model. Mechanobiol.* 17, 1481–1495. doi:10.1007/s10237-018-1040-9

Fu, M., Wang, F., and Lin, G. (2021). Design and Research of Bone Repair Scaffold Based on Two-Way Fluid-Structure Interaction. *Comp. Methods Programs Biomed.* 204, 106055. doi:10.1016/j.cmpb.2021.106055

García-Aznar, J. M., Nasello, G., Hervas-Raluy, S., Pérez, M. Á., and Gómez-Benito, M. J. (2021). Multiscale Modeling of Bone Tissue Mechanobiology. *Bone* 151, 116032. doi:10.1016/j.bone.2021.116032

Giorgi, M., Verbruggen, S. W., and Lacroix, D. (2016). In Silicobone Mechanobiology: Modeling A Multifaceted Biological System. *Wires Syst. Biol. Med.* 8, 485–505. doi:10.1002/wsbm.1356

Granet, C., Laroche, N., Vico, L., Alexandre, C., and Lafage-Proust, M. H. (1998). Rotating-wall Vessels, Promising Bioreactors for Osteoblastic Cell Culture: Comparison with Other 3D Conditions. *Med. Biol. Eng. Comput.* 36, 513–519. doi:10.1007/BF02523224

Grayson, W. L., Bhumiratana, S., Cannizzaro, C., Chao, P.-H. G., Lennon, D. P., Caplan, A. I., et al. (2008). Effects of Initial Seeding Density and Fluid Perfusion Rate on Formation of Tissue-Engineered Bone. *Tissue Eng. A* 14, 1809–1820. doi:10.1089/ten.tea.2007.0255

Guo, R., Lu, S., Page, J. M., Merkel, A. R., Basu, S., Sterling, J. A., et al. (2015). Fabrication of 3D Scaffolds with Precisely Controlled Substrate Modulus and Pore Size by Templated-Fused Deposition Modeling to Direct Osteogenic Differentiation. *Adv. Healthc. Mater.* 4, 1826–1832. doi:10.1002/adhm.201500099

Guyot, Y., Luyten, F. P., Schrooten, J., Papantoniou, I., and Geris, L. (2015). A Three-Dimensional Computational Fluid Dynamics Model of Shear Stress Distribution during Neotissue Growth in a Perfusion Bioreactor. *Biotechnol. Bioeng.* 112, 2591–2600. doi:10.1002/bit.25672

Guyot, Y., Papantoniou, I., Chai, Y. C., Van Bael, S., Schrooten, J., and Geris, L. (2014). A Computational Model for Cell/ECM Growth on 3D Surfaces Using

the Level Set Method: A Bone Tissue Engineering Case Study. *Biomech. Model. Mechanobiol.* 13, 1361–1371. doi:10.1007/s10237-014-0577-5

Guyot, Y., Papantoniou, I., Luyten, F. P., and Geris, L. (2016a). Coupling Curvature-dependent and Shear Stress-Stimulated Neotissue Growth in Dynamic Bioreactor Cultures: A 3D Computational Model of a Complete Scaffold. *Biomech. Model. Mechanobiol.* 15, 169–180. doi:10.1007/s10237-015-0753-2

Guyot, Y., Smeets, B., Odenthal, T., Subramani, R., Luyten, F. P., Ramon, H., et al. (2016b). Immersed Boundary Models for Quantifying Flow-Induced Mechanical Stimuli on Stem Cells Seeded on 3D Scaffolds in Perfusion Bioreactors. *Plos Comput. Biol.* 12, e1005108. doi:10.1371/journal.pcbi.1005108

Hannink, G., and Arts, J. J. C. (2011). Bioresorbability, Porosity and Mechanical Strength of Bone Substitutes: What Is Optimal for Bone Regeneration? *Injury* 42, S22–S25. doi:10.1016/j.injury.2011.06.008

Hendrikson, W. J., Deegan, A. J., Yang, Y., van Blitterswijk, C. A., Verdonschot, N., Moroni, L., et al. (2017). Influence of Additive Manufactured Scaffold Architecture on the Distribution of Surface Strains and Fluid Flow Shear Stresses and Expected Osteochondral Cell Differentiation. *Front. Bioeng. Biotechnol.* 5, 1–11. doi:10.3389/fbioe.2017.00006

Herklotz, M., Prewitz, M. C., Bidan, C. M., Dunlop, J. W. C., Fratzl, P., and Werner, C. (2015). Availability of Extracellular Matrix Biopolymers and Differentiation State of Human Mesenchymal Stem Cells Determine Tissue-like Growth In Vitro. *Biomaterials* 60, 121–129. doi:10.1016/j.biomaterials.2015.04.061

Jahir-Hussain, M. J., Maaruf, N. A., Esa, N. E. F., and Jusoh, N. (2021). The Effect of Pore Geometry on the Mechanical Properties of 3D-Printed Bone Scaffold Due to Compressive Loading. *IOP Conf. Ser. Mater. Sci. Eng.* 1051, 012016. doi:10.1088/1757-899x/1051/1/012016

Janmey, P. A., Fletcher, D. A., and Reinhart-King, C. A. (2020). Stiffness Sensing by Cells. *Physiol. Rev.* 100, 695–724. doi:10.1152/physrev.00013.2019

Jansen, K. A., Donato, D. M., Balcioglu, H. E., Schmidt, T., Danen, E. H. J., and Koenderink, G. H. (2015). A Guide to Mechanobiology: Where Biology and Physics Meet. *Biochim. Biophys. Acta (Bba) - Mol. Cel Res.* 1853, 3043–3052. doi:10.1016/j.bbamcr.2015.05.007

Jungreuthmayer, C., Jaasma, M. J., Al-Munajjed, A. A., Zanghellini, J., Kelly, D. J., and O'Brien, F. J. (2009). Deformation Simulation of Cells Seeded on a Collagen-GAG Scaffold in a Flow Perfusion Bioreactor Using a Sequential 3D CFD-Elastostatics Model. *Med. Eng. Phys.* 31, 420–427. doi:10.1016/j.medengphy.2008.11.003

Kim, S., Uroz, M., Bays, J. L., and Chen, C. S. (2021). Harnessing Mechanobiology for Tissue Engineering. *Dev. Cel* 56, 180–191. doi:10.1016/j.devcel.2020.12.017

Klein-Nulend, J., Bacabac, R. G., Bacabac, R., and Bakker, A. (2012). Mechanical Loading and How it Affects Bone Cells: The Role of the Osteocyte Cytoskeleton in Maintaining Our Skeleton. *eCM* 24, 278–291. doi:10.22203/eCM.v024a20

Klein-Nulend, J., Bacabac, R. G., Veldhuijzen, J. P., and Van Loon, J. J. W. A. (2003). Microgravity and Bone Cell Mechanosensitivity. *Adv. Space Res.* 32, 1551–1559. doi:10.1016/S0273-1177(03)90395-4

Laurent, C. P., Latil, P., Durville, D., Rahouadj, R., Geindreau, C., Orgéas, L., et al. (2014). Mechanical Behaviour of a Fibrous Scaffold for Ligament Tissue Engineering: Finite Elements Analysis vs. X-ray Tomography Imaging. *J. Mech. Behav. Biomed. Mater.* 40, 222–233. doi:10.1016/j.jmbbm.2014.09.003

Li, D., Tang, T., Lu, J., and Dai, K. (2009). Effects of Flow Shear Stress and Mass Transport on the Construction of a Large-Scale Tissue-Engineered Bone in a Perfusion Bioreactor. *Tissue Eng. Part A* 15, 2773–2783. doi:10.1089/ten.tea.2008.0540

Lin, X., Patil, S., Gao, Y.-G., and Qian, A. (2020). The Bone Extracellular Matrix in Bone Formation and Regeneration. *Front. Pharmacol.* 11, 1–15. doi:10.3389/fphar.2020.00757

Mccoy, R. J., Jungreuthmayer, C., and O'Brien, F. J. (2012). Influence of Flow Rate and Scaffold Pore Size on Cell Behavior During Mechanical Stimulation in a Flow Perfusion Bioreactor. *Biotechnol. Bioeng.* 109, 1583–1594. doi:10.1002/bit.24424

Melchels, F. P. W., Tonnarelli, B., Olivares, A. L., Martin, I., Lacroix, D., Feijen, J., et al. (2011). The Influence of the Scaffold Design on the Distribution of Adhering Cells After Perfusion Cell Seeding. *Biomaterials* 32, 2878–2884. doi:10.1016/j.biomaterials.2011.01.023

Milan, J.-L., Planell, J. A., and Lacroix, D. (2009). Computational Modelling of the Mechanical Environment of Osteogenesis Within a Polylactic Acid-Calcium

Phosphate Glass Scaffold. *Biomaterials* 30, 4219–4226. doi:10.1016/j.biomaterials.2009.04.026

Munch, E., Saiz, E., Tomsia, A. P., and Deville, S. (2009). Architectural Control of Freeze-Cast Ceramics Through Additives and Templating. *J. Am. Ceram. Soc.* 92, 1534–1539. doi:10.1111/j.1551-2916.2009.03087.x

Naqvi, S. M., and McNamara, L. M. (2020). Stem Cell Mechanobiology and the Role of Biomaterials in Governing Mechanotransduction and Matrix Production for Tissue Regeneration. *Front. Bioeng. Biotechnol.* 8, 1–27. doi:10.3389/fbioe.2020.597661

Nasello, G., Vautrin, A., Pitocchi, J., Wesseling, M., Kuiper, J. H., Pérez, M. Á., et al. (2021). Mechano-driven Regeneration Predicts Response Variations in Large Animal Model Based on Scaffold Implantation Site and Individual Mechano-Sensitivity. *Bone* 144, 115769. doi:10.1016/j.bone.2020.115769

Nava, M. M., Raimondi, M. T., and Pietrabissa, R. (2013). A Multiphysics 3D Model of Tissue Growth Under Interstitial Perfusion in a Tissue-Engineering Bioreactor. *Biomech. Model. Mechanobiol.* 12, 1169–1179. doi:10.1007/s10237-013-0473-4

Olivares, A. L., Marsal, È., Planell, J. A., and Lacroix, D. (2009). Finite Element Study of Scaffold Architecture Design and Culture Conditions for Tissue Engineering. *Biomaterials* 30, 6142–6149. doi:10.1016/j.biomaterials.2009.07.041

Ouyang, P., Dong, H., He, X., Cai, X., Wang, Y., Li, J., et al. (2019). Hydromechanical Mechanism behind the Effect of Pore Size of Porous Titanium Scaffolds on Osteoblast Response and Bone Ingrowth. *Mater. Des.* 183, 108151. doi:10.1016/j.matdes.2019.108151

Paluch, E. K., Nelson, C. M., Biais, N., Fabry, B., Moeller, J., Pruitt, B. L., et al. (2015). Mechanotransduction: Use the Force(s). *BMC Biol.* 13, 1–14. doi:10.1186/s12915-015-0150-4

Panadero, J. A., Vikingsson, L., Gomez Ribelles, J. L., Lanceros-Mendez, S., and Sencadas, V. (2015). In Vitromechanical Fatigue Behavior of Poly-Ɛ-Caprolactone Macroporous Scaffolds for Cartilage Tissue Engineering: Influence of Pore Filling by a Poly(vinyl Alcohol) Gel. *J. Biomed. Mater. Res.* 103, 1037–1043. doi:10.1002/jbm.b.33276

Panseri, S., Montesi, M., Hautcoeur, D., Dozio, S. M., Chamary, S., De Barra, E., et al. (2021). Bone-like Ceramic Scaffolds Designed with Bioinspired Porosity Induce a Different Stem Cell Response. *J. Mater. Sci. Mater. Med.* 32, 3. doi:10.1007/s10856-020-06486-3

Pourhaghgouy, M., Zamanian, A., Shahrezaee, M., and Masouleh, M. P. (2016). Physicochemical Properties and Bioactivity of Freeze-Cast Chitosan Nanocomposite Scaffolds Reinforced with Bioactive Glass. *Mater. Sci. Eng. C* 58, 180–186. doi:10.1016/j.msec.2015.07.065

Prochor, P., and Gryko, A. (2021). Numerical Analysis of the Influence of Porosity and Pore Geometry on Functionality of Scaffolds Designated for Orthopedic Regenerative Medicine. *Materials* 14, 109–119. doi:10.3390/ma14010109

Ribeiro, J. F. M., Oliveira, S. M., Alves, J. L., Pedro, A. J., Reis, R. L., Fernandes, E. M., et al. (2017). Structural Monitoring and Modeling of the Mechanical Deformation of Three-Dimensional Printed Poly(ε -caprolactone) Scaffolds. *Biofabrication* 9, 025015. doi:10.1088/1758-5090/aa698e

Rüberg, T., and Aznar, J. M. G. (2016). Numerical Simulation of Solid Deformation Driven by Creeping Flow Using an Immersed Finite Element Method. *Adv. Model. Simul. Eng. Sci.* 3, 9. doi:10.1186/s40323-016-0061-0

Rubert, M., Vetsch, J. R., Lehtoviita, I., Sommer, M., Zhao, F., Studart, A. R., et al. (2020). Scaffold Pore Geometry Guides Gene Regulation and Bone-like Tissue Formation in Dynamic Cultures. *Tissue Eng. Part A*. doi:10.1089/ten.TEA.2020.0121

Sandino, C., and Lacroix, D. (2011). A Dynamical Study of the Mechanical Stimuli and Tissue Differentiation Within a CaP Scaffold Based on Micro-CT Finite Element Models. *Biomech. Model. Mechanobiol.* 10, 565–576. doi:10.1007/s10237-010-0256-0

Selig, M., Lauer, J. C., Hart, M. L., and Rolauffs, B. (2020). Mechanotransduction and Stiffness-Sensing: Mechanisms and Opportunities to Control Multiple Molecular Aspects of Cell Phenotype as a Design Cornerstone of Cell-Instructive Biomaterials for Articular Cartilage Repair. *Ijms* 21, 5399. doi:10.3390/ijms21155399

Serrano-Alcalde, F., García-Aznar, J. M., and Gómez-Benito, M. J. (2017). The Role of Nuclear Mechanics in Cell Deformation Under Creeping Flows. *J. Theor. Biol.* 432, 25–32. doi:10.1016/j.jtbi.2017.07.028

Sikavitsas, V. I., Bancroft, G. N., and Mikos, A. G. (2002). Formation of Three-Dimensional Cell/polymer Constructs for Bone Tissue Engineering in a Spinner Flask and a Rotating Wall Vessel Bioreactor. *J. Biomed. Mater. Res.* 62, 136–148. doi:10.1002/jbm.10150

Tang, Y., Xiong, Y., Park, S.-i., and Rosen, D. W. (2020). Universal Material Template for Heterogeneous Objects with Applications to Additive Manufacturing. *Computer-Aided Des.* 129, 102929. doi:10.1016/j.cad.2020.102929in, and

Van Bael, S., Chai, Y. C., Truscello, S., Moesen, M., Kerckhofs, G., Van Oosterwyck, H., et al. (2012). The Effect of Pore Geometry on the In Vitro Biological Behavior of Human Periosteum-Derived Cells Seeded on Selective Laser-Melted Ti6Al4V Bone Scaffolds. *Acta Biomater.* 8, 2824–2834. doi:10.1016/j.actbio.2012.04.001

Wittkowske, C., Reilly, G. C., Lacroix, D., and Perrault, C. M. (2016). In Vitro Bone Cell Models: Impact of Fluid Shear Stress on Bone Formation. *Front. Bioeng. Biotechnol.* 4, 87. doi:10.3389/fbioe.2016.00087

Xiong, Y., Duong, P. L. T., Wang, D., Park, S.-I., Ge, Q., Raghavan, N., et al. (2019). Data-driven Design Space Exploration and Exploitation for Design for Additive Manufacturing. *J. Mech. Des. Trans. ASME* 141, 1–12. doi:10.1115/1.4043587

Yamashita, T., Kollmannsberger, P., Mawatari, K., Kitamori, T., and Vogel, V. (2016). Cell Sheet Mechanics: How Geometrical Constraints Induce the Detachment of Cell Sheets from Concave Surfaces. *Acta Biomater.* 45, 85–97. doi:10.1016/j.actbio.2016.08.044

Zermatten, E., Vetsch, J. R., Ruffoni, D., Hofmann, S., Müller, R., and Steinfeld, A. (2014). Micro-Computed Tomography Based Computational Fluid Dynamics for the Determination of Shear Stresses in Scaffolds Within A Perfusion Bioreactor. *Ann. Biomed. Eng.* 42, 1085–1094. doi:10.1007/s10439-014-0981-0

Zhang, X.-Y., Fang, G., Leeflang, S., Zadpoor, A. A., and Zhou, J. (2019). Topological Design, Permeability and Mechanical Behavior of Additively Manufactured Functionally Graded Porous Metallic Biomaterials. *Acta Biomater.* 84, 437–452. doi:10.1016/j.actbio.2018.12.013

Zhao, F., Lacroix, D., Ito, K., van Rietbergen, B., and Hofmann, S. (2020a). Changes in Scaffold Porosity during Bone Tissue Engineering in Perfusion Bioreactors Considerably Affect Cellular Mechanical Stimulation for Mineralization. *Bone Rep.* 12, 100265. doi:10.1016/j.bonr.2020.100265

Zhao, F., Melke, J., Ito, K., Rietbergen, B. Van., and Hofmann, S. (2019). A Multiscale Computational Fluid Dynamics Approach to Simulate the Micro-fluidic Environment within a Tissue Engineering Scaffold with Highly Irregular Pore Geometry. *Biomech. Model. Mechanobiol* 18 (6), 1965–1977. doi:10.1007/s10237-019-01188-4

Zhao, F., Rietbergen, B., Ito, K., and Hofmann, S. (2020b). Fluid Flow-induced Cell Stimulation in Bone Tissue Engineering Changes Due to Interstitial Tissue Formation In Vitro. *Int. J. Numer. Meth Biomed. Engng* 36, 1–12. doi:10.1002/cnm.3342

Zhao, F., Vaughan, T. J., and McNamara, L. M. (2016). Quantification of Fluid Shear Stress in Bone Tissue Engineering Scaffolds with Spherical and Cubical Pore Architectures. *Biomech. Model. Mechanobiol.* 15, 561–577. doi:10.1007/s10237-015-0710-0